Antioxidants & redox signaling (2011.Oct) 15巻8号:2109～2120.

Critical roles of cold shock domain protein A as an endogenous angiogenesis inhibitor in skeletal muscle

Saito Y, Nakagami H, Azuma N, Hirata S, Sanada F, Taniyama Y, Morishita R, Kaneda Y, Sasajima T

ANTIOXIDANTS & REDOX SIGNALING
Volume 15, Number 8, 2011

DOI: 10.1089/ars.2010.3714

ORIGINAL RESEARCH COMMUNICATION

Critical Roles of Cold Shock Domain Protein A as an Endogenous Angiogenesis Inhibitor in Skeletal Muscle

Yukihiro Saito,[1] Hironori Nakagami,[2] Nobuyoshi Azuma,[1] Satoshi Hirata,[1] Fumihiro Sanada,[3] Yoshiaki Taniyama,[3] Ryuichi Morishita,[3] Yasufumi Kaneda,[4] and Tadahiro Sasajima[1]

Abstract

Angiogenesis is regulated by the local balance between angiogenic stimulators and inhibitors and is maintained by muscle-derived angiogenic factors in ischemic tissues. ***Aims:*** Our objectives were to investigate the effect of cold shock domain protein A (CSDA) as an endogenous angiogenesis inhibitor and to develop a novel strategy of therapeutic angiogenesis by blocking CSDA expression. ***Results:*** In human skeletal muscle cells, CSDA was upregulated during hypoxia when cells were damaged and apoptosis was induced. CSDA expression could repress the activity of hypoxia inducible factor-1α and nuclear factor κB, because CSDA can competitively bind the hypoxia response element and the nuclear factor κB-binding element. As a result, vascular endothelial growth factor-A, interleukin-6, and interleukin-8 secretions from skeletal muscle cells were decreased. Further, CSDA depletion increased the secretion level of these angiogenic factors. In a hindlimb ischemia model, transfer of short-hairpin RNA targeting CSDA ameliorated ischemia without direct transfer of angiogenic factors. In this ischemic tissue, vascular endothelial growth factor-A, interleukin-6, and CXCL2 protein levels were increased. ***Innovation and Conclusion:*** CSDA appears to play a critical role as an endogenous angiogenesis inhibitor in skeletal muscle, and RNA interference targeting of CSDA is a promising gene therapy strategy for treating peripheral arterial disease. *Antioxid. Redox Signal.* 15, 2109–2120.

Introduction

THERAPEUTIC ANGIOGENESIS is a promising strategy for treating peripheral arterial disease (PAD), in addition to pharmacotherapy, percutaneous transluminal angioplasty, and vascular surgery. Over the past several years, angiogenic growth factors, such as vascular endothelial growth factor (VEGF)-A (7), fibroblast growth factor (2), and angiopoietin-1 (6), have been utilized in gene therapies designed to provide therapeutic angiogenesis for PAD. Although these molecules powerfully promote cellular proliferation and migration *in vitro*, their utility is not sufficient for clinical use. Clinical success has been limited to a small group of selected patients. Unfortunately, a randomized, double-blind, placebo-controlled trial of this strategy failed to show a significant benefit (7). The long-term safety and efficacy of these therapies remain unclear, and there is little scientific evidence to resolve these questions. Novel strategies are therefore required to achieve clinical benefit. Further, angiogenesis is regulated by a local balance between angiogenesis stimulators and inhibitors (25); however, the detailed mechanisms responsible for this balance, especially the negative regulation of angiogenesis, remain unclear.

We recently identified a new molecule, cold shock domain protein A (CSDA), which is an angiogenic modulator (20). CSDA is a DNA-binding protein that especially binds CT-rich DNA sequences (26). We found that in endothelial cells, CSDA can bind to the hypoxia response element (HRE) contained in the VEGF promoter region and to the serum response element (SRE), the final target of the Ras/extracellular signal-regulated kinase signal, and repress the activation of these elements as a blocker. CSDA competes with hypoxia inducible factor (HIF)-1α and Elk-1, repressing the expression of VEGF-A and endothelial cell proliferation, respectively (Supplementary Fig. S1; Supplementary Data available online at www.liebertonline.com/ars). Further, we found that CSDA is expressed in normal skeletal muscle, but the function of CSDA in this tissue is not known. Recently, the importance of muscle-derived angiogenic factors in the neovascularization of ischemic skeletal muscle was recognized (30).

In the present study, we tested the hypothesis that CSDA plays an important role as an endogenous angiogenesis inhibitor by repressing the expression or function of angiogenic factors in skeletal muscle. Further, the depletion of CSDA expression with a knockdown strategy may improve the

[1]Department of Surgery, Asahikawa Medical University, Asahikawa, Hokkaido, Japan.
[2]Department of Epigenetic and Vascular Medicine, United Graduate School of Child Development, Osaka University, Suita, Osaka, Japan.
[3]Division of Clinical Gene Therapy and [4]Division of Gene Therapy Science, Graduate School of Medicine, Osaka University, Suita, Osaka, Japan.

angiogenic response in ischemic tissues through the modulation of endogenous angiogenic factors. The goals of the present study were to investigate the effect of CSDA as an endogenous angiogenesis inhibitor during hypoxic (ischemic) conditions and to develop a novel gene therapy strategy for PAD using RNA interference (RNAi) to target CSDA.

Results

Effect of hypoxia on CSDA expression and SkMC apoptosis

Skeletal muscle cells (SkMCs) were cultured under hypoxic conditions for 7 days, and CSDA expression was examined at five time points. *CSDA* messenger RNA (mRNA) expression was downregulated at 1 day of hypoxia and then upregulated, especially by day 7 ($n=4$; Fig. 1A). The protein levels of CSDA decreased up to 3 days of hypoxia but then increased rapidly at day 7 ($n=4$; Fig. 1B and C). To understand the differences between the early phase (up to 3 days) and late phase (after 3 days) of hypoxia in CSDA expression, we measured the mitochondrial transmembrane potential and performed terminal deoxy nucleotidyl transferase dUTP nick end labeling (TUNEL) analysis of SkMCs under hypoxic conditions and performed western blot analysis of cytochrome *c*, because disruption of the mitochondrial transmembrane potential and translocation of cytochrome *c* are some of the earliest intracellular indicators of apoptosis. Over 3 days of hypoxia, the mitochondrial transmembrane potential was disrupted (Fig. 1D, green-colored cells), and the SkMCs were in disarray (Fig. 1E). Further, western blot of cytochrome *c* indicated that hypoxic conditions triggered the release of cytochrome *c* from the mitochondria into the cytosol (Fig. 1F). The cells were TUNEL positive at day 7 of hypoxia (Fig. 1E, brown-colored cells). At day 7, CSDA expression was detected in caspase 3-positive and TUNEL-positive SkMCs by immunofluorescence staining (Fig. 2A and B). When SkMCs were treated by apoptosis inducers under normoxic conditions for 3 days, the mitochondrial transmembrane potential was disrupted (Fig. 2C), and TUNEL analysis was positive for these cells (Fig. 2D). Further, CSDA was induced by treatment with apoptosis inducers for 3 days under normoxic conditions (Fig. 2E and F). We also found that after 3 days of hypoxia, the cell population was composed of many apoptotic cells with a few terminal apoptotic

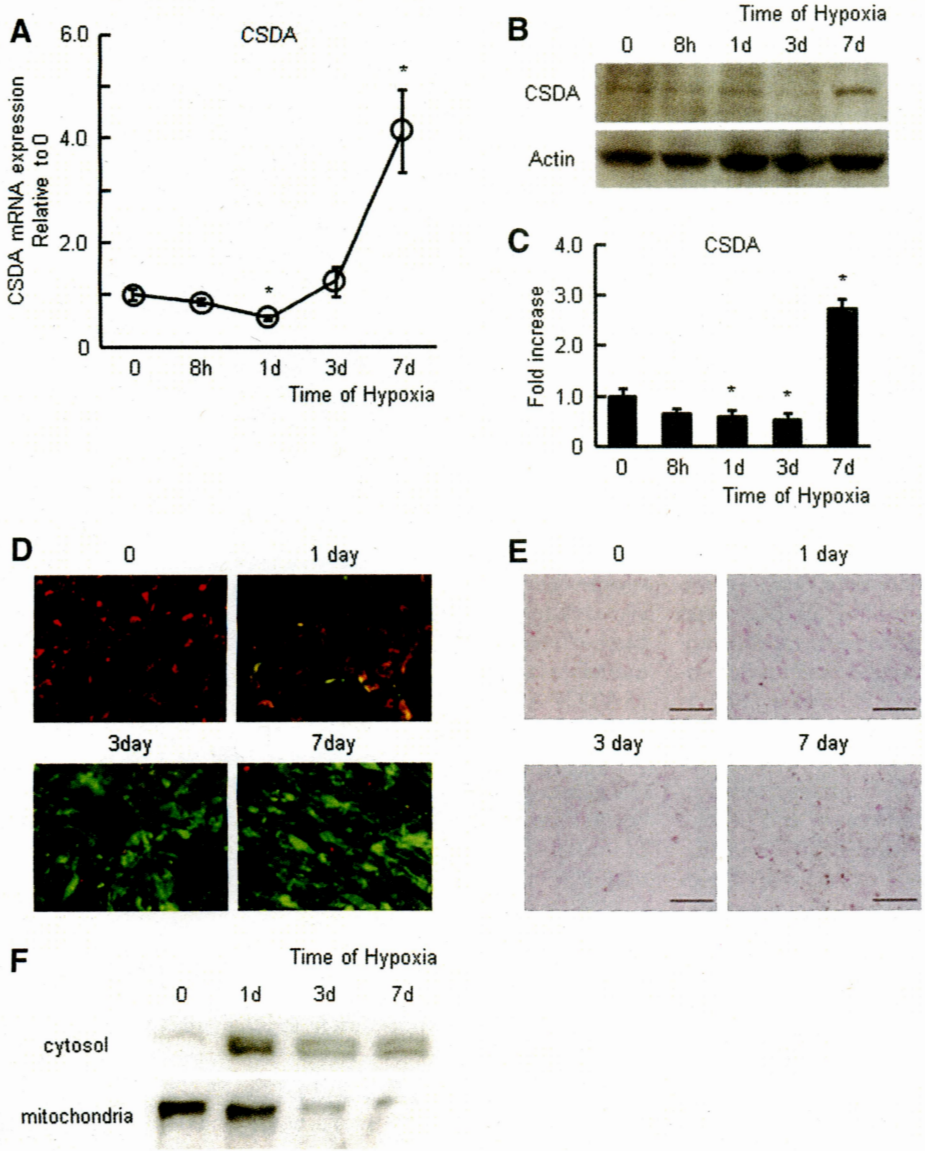

FIG. 1. Hypoxia modulates CSDA expression and induces SkMC apoptosis. (A) Expression of endogenous *CSDA* in SkMCs after 0 h, 8 h, and 1, 3, and 7 days of hypoxia. $n=4$; $^*p<0.05$ *versus* 0 h. **(B)** Typical western blots of endogenous CSDA after 0 h, 8 h, and 1, 3, and 7 days of hypoxia. **(C)** Fold increase in endogenous CSDA expression shown in **B** compared with 0 h in SkMCs. $n=4$; $^*p<0.05$ *versus* 0 h. **(D)** Representative images of the mitochondrial transmembrane potential in SkMCs during hypoxic conditions. In healthy cells, fluorescent molecules aggregated inside the mitochondria and fluoresced red (until after 1 day of hypoxia). In apoptotic cells, fluorescent molecules remained in the cytoplasm and fluoresced green (after 3 days of hypoxia) (magnification: 200×). **(E)** Representative pictures of TUNEL analysis of SkMCs under hypoxic conditions, followed by counterstaining with methyl green–pyronin. Healthy cells are pink, and apoptotic cells are brown. Scale bar = 100 μm. **(F)** Typical western blots of cytochrome *c* after 0, 1, 3, and 7 days of hypoxia. CSDA, cold shock domain protein A; SkMC, skeletal muscle cell.

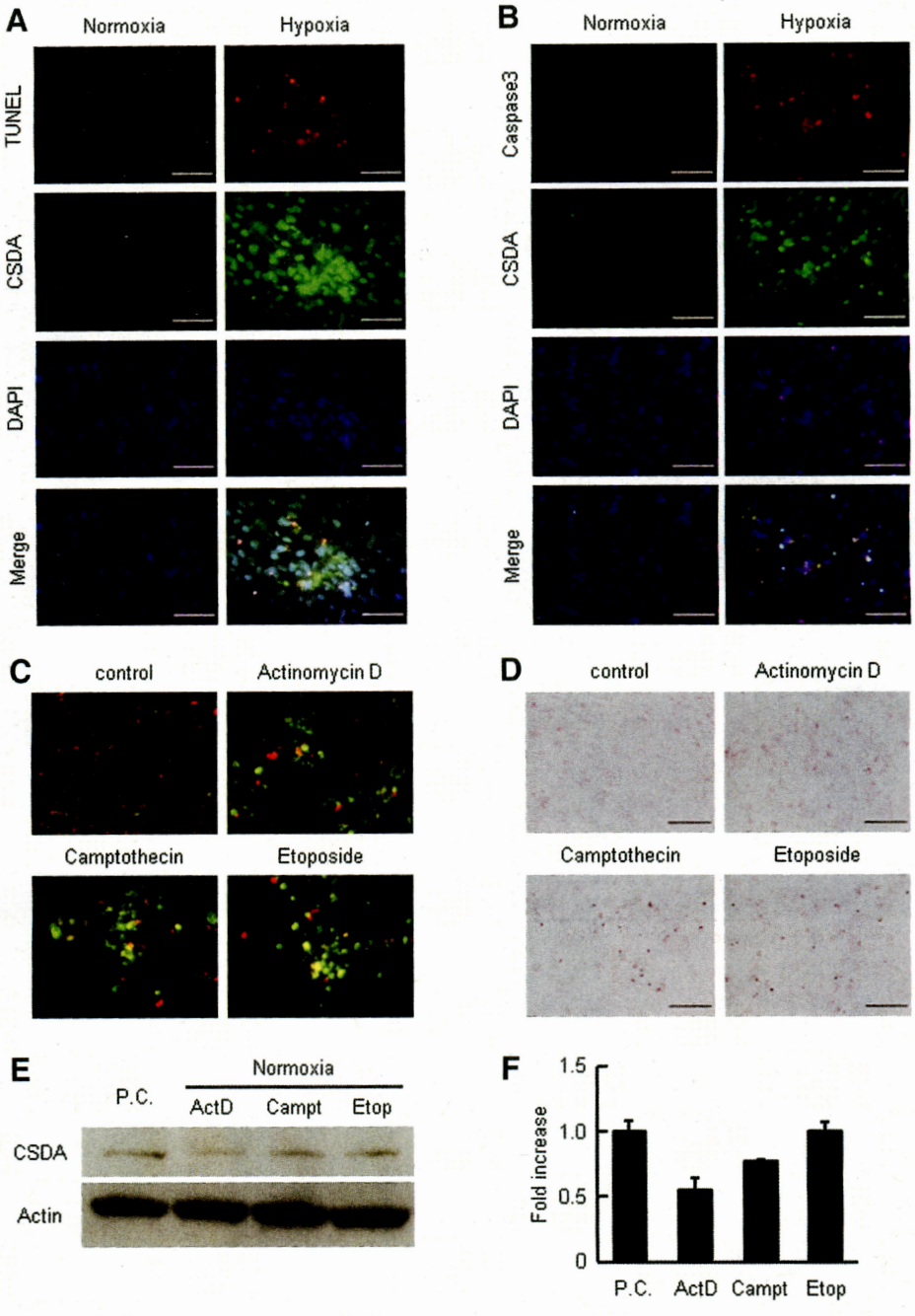

FIG. 2. Apoptosis induces CSDA in SkMCs. (A, B) Representative pictures of double immunofluorescent stains for TUNEL (A) or caspase 3 **(B)** (red) and CSDA (green) in SkMCs after 7 days of hypoxia. Nuclei were stained by DAPI (blue). Scale bar = 100 μm. **(C)** Representative images of the mitochondrial transmembrane potential in SkMCs treated by apoptosis inducers. In healthy cells, fluorescent molecules aggregated inside the mitochondria and fluoresced red. In apoptotic cells, the fluorescent molecules remained in the cytoplasm and fluoresced green (magnification: 200×). **(D)** Representative pictures of TUNEL analysis of SkMCs treated by apoptosis inducers, followed by counterstaining with methyl green–pyronin. Healthy cells are pink, and apoptotic cells are brown. Scale bar = 100 μm. **(E)** Typical western blot of CSDA in SkMCs treated by apoptosis inducers. These cultures were incubated under normoxic conditions for 3 days. P.C. indicates cell lysates that overexpressed CSDA under normoxic conditions. **(F)** Fold increase in endogenous CSDA expression shown in Figure 1E compared with the positive control; $n = 4$. There was no significant change compared with the positive control. ActD, actinomycin D; Campt, camptothecin; DAPI, 4′,6-diamino-2-phenylindole; Etop, etoposide; P.C., positive control.

or necrotic cells as assessed by staining (Supplementary Fig. S2A and B). Autophagy of SkMCs was assessed by western blot of LC-3 and Atg-12. These autophagy markers were increased at 1 day of hypoxia, but then decreased rapidly (Supplementary Fig. S2C). These results suggest that CSDA expression changed under hypoxic conditions and was correlated with cell damage (apoptosis and, to a lesser extent, necrosis).

Regulation of VEGF-A secretion from SkMCs by CSDA

In SkMCs cultured under hypoxic conditions, the mRNA expression levels of HIF-1α were strongly upregulated at day 1 of hypoxia ($n = 4$; Fig. 3A) and those of VEGF-A were upregulated at 3 days of hypoxia, after which they decreased significantly ($n = 4$; Fig. 3B). The corresponding protein levels changed in parallel with mRNA levels (Fig. 3C–E). These changes in VEGF-A and HIF-1α expression seemed to behave in the opposite direction of that of CSDA.

Previously, we and others reported that CSDA can inhibit VEGF-A promoter activity by competitively binding to HRE in endothelial cells (3). In SkMCs, VEGF promoter activity significantly increased under hypoxic conditions, but overexpression of CSDA significantly repressed this increase when compared with control hypoxia ($p < 0.05$; Fig. 3F). Under normoxic conditions, depletion of CSDA by shCSDA increased VEGF promoter activity significantly up to the level induced by hypoxia. Further, under hypoxic conditions, shCSDA increased VEGF promoter activity far above the shSC level of hypoxia ($p < 0.05$; Fig. 3G). Overexpressed CSDA decreased VEGF-A secretion ($p < 0.05$; Fig. 3H), and depletion of CSDA expression significantly increased

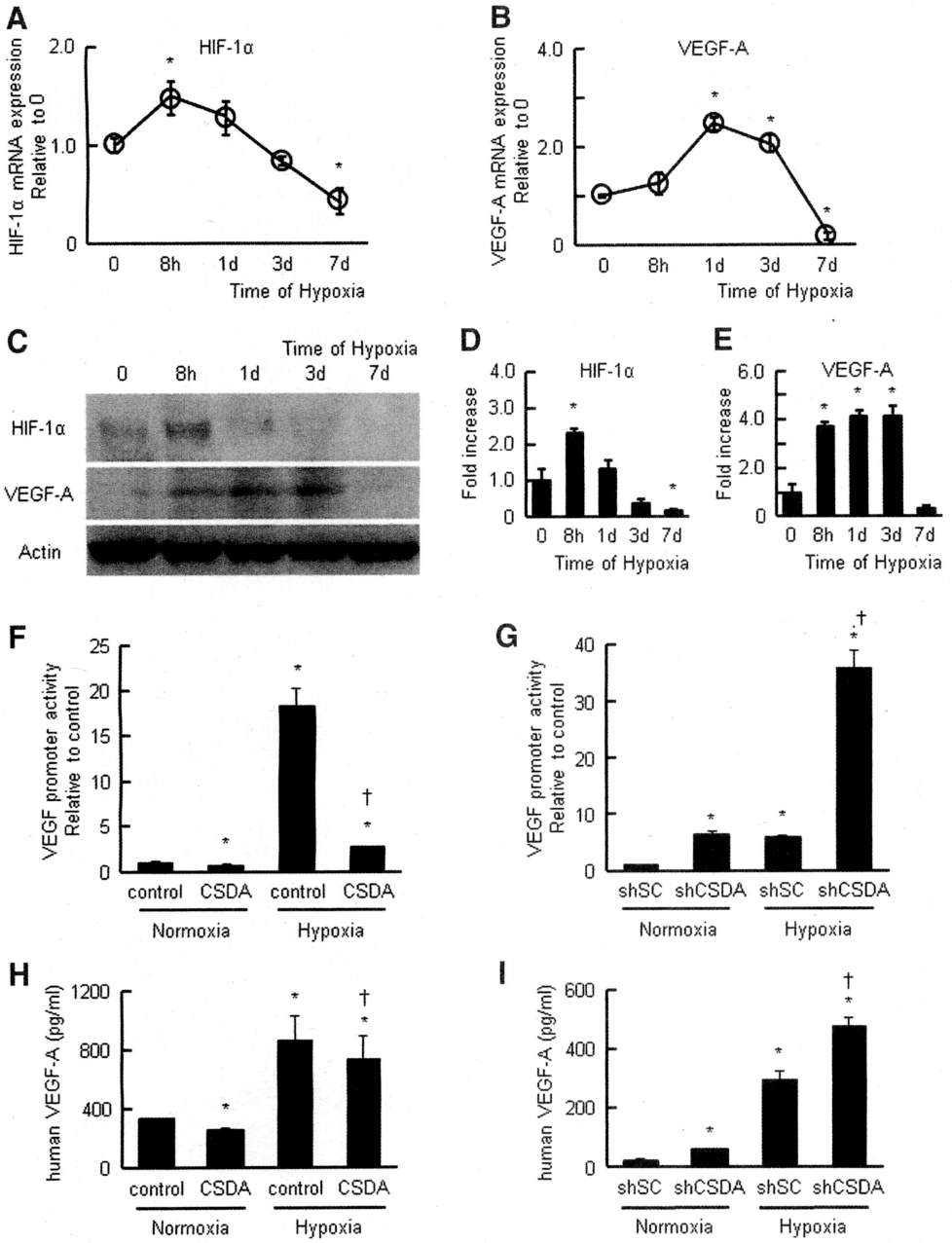

FIG. 3. CSDA regulates VEGF-A secretion from SkMCs. (A, B) Expression of endogenous *HIF-1α* **(A)** and *VEGF-A* **(B)** of SkMCs after 0 h, 8 h, and 1, 3, and 7 days of hypoxia. $n=4$; $^*p<0.05$ *versus* 0 h. **(C)** Typical western blots of endogenous HIF-1α (nuclear extracts) and VEGF-A (whole-cell lysates) after 0 h, 8 h, and 1, 3, and 7 days of hypoxia. **(D, E)** Fold increase in endogenous HIF-1α **(D)** and VEGF-A **(E)** expression shown in Figure 3C compared with 0 h. $n=4$; $^*p<0.05$ *versus* 0 h. **(F, G)** Effect of CSDA plasmid **(F)** or shCSDA **(G)** on VEGF promoter activity in SkMCs under normoxic or hypoxic conditions for 3 days. **(H, I)** Effect of CSDA plasmid **(H)** or shCSDA **(I)** on VEGF-A secretion from SkMCs under normoxic or hypoxic conditions for 3 days. $n=6$; $^*p<0.05$ *versus* control or shSC of normoxia; $^\dagger p<0.05$ *versus* control or shSC of hypoxia. GFP plasmid or shSC plasmid was transfected as a control. GFP, green fluorescence protein; HIF, hypoxia inducible factor; VEGF, vascular endothelial growth factor.

VEGF-A secretion ($p<0.05$; Fig. 3I) when compared with the control or shSC. Clearly, VEGF secretion was not strongly affected by overexpression of CSDA when compared with the change in VEGF promoter activity. These results suggest that another mechanism of regulation of VEGF-A may exist; indeed, HIF-independent regulation of VEGF-A has been previously reported (1). However, depletion of CSDA resulted in a 60% upregulation of VEGF-A secretion under hypoxic conditions. These data suggest that HIF-1α expression and activity are possibly affected by hypoxia-induced CSDA competition, resulting in the repression of VEGF-A secretion.

DNA binding of CSDA to the NFκB-binding element and regulation of NFκB activity

Nuclear factor κB (NFκB) is an important molecule for angiogenesis, because NFκB activation has the potential to induce HIF-1α (10, 19), and NFκB activation is followed by the activation of several angiogenic cytokines (11, 13). Because cold shock domain (CSD) proteins can bind CT-rich DNA sequences (26), we tested the hypothesis that CSDA can directly bind the NFκB-binding element (BE) to repress the activation of several cytokines (Supplementary Fig. S3). Immunofluorescence staining of SkMCs by anti-p65 antibody demonstrated that p65 was translocated into the nucleus at 1 day of hypoxia (Fig. 4A). The expression of NFκB mRNA in SkMCs was upregulated at day 1, as quantified by real-time quantitative PCR ($n=4$; Fig. 4B). NFκB activation can be quantified by the phosphorylation of p65 at multiple serine sites by some protein kinases (16). NFκB (p65) was phosphorylated in the nuclei of SkMCs under hypoxic conditions at day 1, whereas the total NFκB protein level was not altered by hypoxia (Fig. 4C). These results suggest that NFκB in SkMCs was activated by hypoxia. Gel mobility shift assays

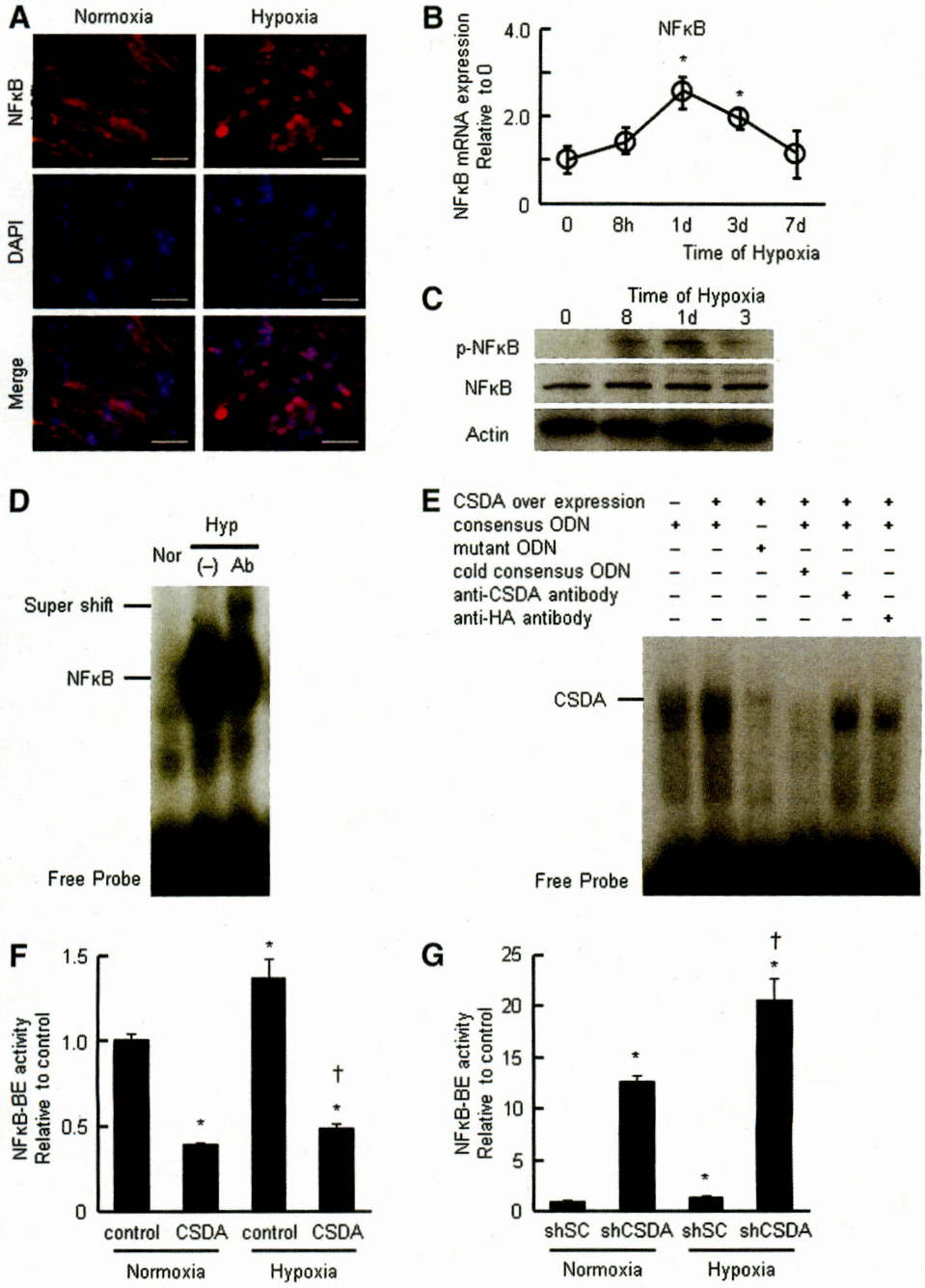

FIG. 4. CSDA binds the NFκB-binding element and regulates *NFκB* activity. (A) Representative immunofluorescence staining image of SkMCs for NFκB (p65) under normoxic (*left panels*) and hypoxic (day 3, *right panels*) conditions. Scale bar = 200 μm. **(B)** Expression of endogenous *NFκB* (p65) in SkMCs after 0 h, 8 h, and 1, 3, and 7 days of hypoxia. $n = 4$; $^{*}p < 0.05$ *versus* 0 h. **(C)** Typical western blots of endogenous phospho-NFκB (p65) and total NFκB (p65) in nuclear extracts of SkMCs after 0 h, 8 h, and 1 and 3 days of hypoxia. **(D)** Representative image of a gel retardation assay for NFκB binding to the NFκB-BE. **(E)** Representative image of a gel retardation assay for CSDA binding to the NFκB-BE. **(F, G)** Effect of CSDA plasmid **(F)** or shCSDA **(G)** on NFκB-BE activity in SkMCs during normoxic or hypoxic conditions for 1 day. $n = 6$; $^{*}p < 0.05$ *versus* control or shSC of normoxia; $^{\dagger}p < 0.05$ *versus* control or shSC of hypoxia. GFP plasmid or shSC plasmid was transfected as a control. NFκB-BE, nuclear factor κB-binding element.

demonstrated that hypoxia increases NFκB DNA-binding activity, and this band was supershifted using p65 antibody (Fig. 4D). Overexpression of the CSDA gene increased specific binding to the consensus NFκB-BE, but not to mutant NFκB-BE. Further, preincubation of nuclear extract with anti-CSDA antibody blocked the formation of the CSDA-NFκB-BE complex (Fig. 4E), as previously reported (3, 4). These results indicate that CSDA can compete with NFκB and directly bind the NFκB-BE. We further examined the effect of CSDA expression on NFκB-BE activity in SkMCs using an NFκB-BE-luciferase reporter gene. Overexpressed CSDA significantly decreased hypoxia-induced NFκB-BE activity to the level of normoxia ($p < 0.05$; Fig. 4F), and depletion of CSDA by shCSDA significantly increased NFκB-BE activity over the normoxia level ($p < 0.05$; Fig. 4G).

Regulation of IL-6 and IL-8 secretion from SkMCs by CSDA

Next, we examined the expression and secretion of interleukin (IL)-6 and IL-8 from SkMCs, because NFκB can regulate these angiogenic cytokines (5) and it has been reported that these cytokines are secreted from skeletal muscle (18, 30). The expression levels of *IL-6* and *IL-8* mRNA were upregulated at day 1 of hypoxia, as quantified by real-time quantitative PCR ($n = 4$; Fig. 5A and B). Overexpressed CSDA decreased IL-6 and IL-8 secretion when compared with the control ($p < 0.05$; Fig. 5C and D), and depletion of CSDA significantly increased IL-6 and IL-8 secretion when compared with shSC ($p < 0.05$; Fig. 5E and F). The changes in NFκB, IL-6, and IL-8 expression levels appeared to be similar to those of

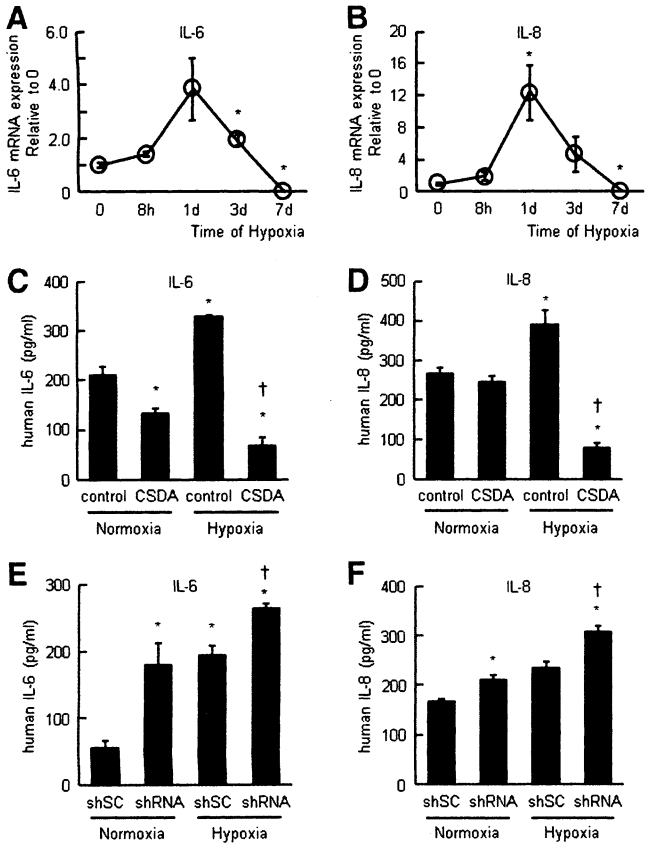

FIG. 5. CSDA regulates IL-6 and IL-8 secretions from SkMCs. (A, B) Expression of endogenous *IL-6* **(A)** and *IL-8* **(B)** in SkMCs after 0 h, 8 h, and 1, 3, and 7 days of hypoxia. $n=4$; $^*p<0.05$ *versus* 0 h. **(C, D)** Effect of CSDA plasmid on IL-6 **(C)** or IL-8 **(D)** secretion from SkMCs during normoxic or hypoxic conditions for 1 day. **(E, F)** Effect of shCSDA on IL-6 **(E)** or IL-8 **(F)** secretion from SkMCs during normoxia or hypoxia for 1 day. $n=6$; $^*p<0.05$ *versus* control or shSC of normoxia; $^\dagger p<0.05$ *versus* control or shSC of hypoxia. GFP plasmid or shSC plasmid was transfected as a control. IL, interleukin.

HIF-1α and VEGF-A and behaved in the opposite direction of that of CSDA.

Effects of CSDA on in vitro *angiogenesis*

To confirm the effect of CSDA on angiogenesis, a tube formation assay using an angiogenesis assay kit was performed with endothelial aortic cells. The tube-like structures were decreased in the CSDA group, but were increased in the shCSDA group (Fig. 6A). Quantitative analysis of the total tube length confirmed that there was a significant increase in tube formation by gene transfer of shCSDA when compared with the group with no treatment (Fig. 6B).

These results suggest that CSDA can regulate the angiogenesis response induced by VEGF-A, IL-6, and IL-8 secretion in SkMCs *via* blocking HRE and NFκB-BE activation.

Gene therapy with RNAi targeting CSDA in vivo

On the basis of our *in vitro* data, we assessed the hypothesis that Csda knockdown would stimulate angiogenesis and alter ischemia. To test this concept, a hindlimb ischemia mouse model was created, and the shCSDA plasmid was transfected into ischemic muscle tissue using the ultrasound-sonoporation method (27). In the control group, the expression of *CSDA* mRNA was downregulated at day 7 but was upregulated at day 25. Depletion of *Csda* by shCSDA resulted in 78.8% repression of *CSDA* mRNA level at day 25 ($n=4$; Fig. 7A).

Figure 7B shows representative laser Doppler imaging (LDI) images of hindlimb blood flow at days 4 and 28 after surgery, and only the shCSDA group was observed to have high perfusion in the operated side limb (Fig. 7B, white arrow; images of other groups not shown). Depletion of CSDA by shCSDA resulted in a significant improvement in the ratio of ischemic/nonischemic limb blood flow from 25 days after surgery, although serial LDI examinations revealed the continuity of ischemia in the other groups ($p<0.05$; Fig. 7C). To investigate the degree of angiogenesis at the microcirculation level, histological sections were harvested from ischemic skeletal tissues and stained with the endothelial cell markers von Willebrand Factor (Fig. 7D) and CD31 (Fig. 7E). The capillary density in these sections was significantly increased in the shCSDA group compared with the control group ($p<0.05$; Fig. 7F). In the control group, the CSDA expression was detected in SkMCs but not in endothelial cells, whereas expression of CSDA protein was downregulated by gene transfer of shCSDA (Fig. 8A). We investigated whether depletion of CSDA could accelerate the angiogenic process *in vivo* by analyzing ischemic muscle tissues at days 0, 7, and 25 after surgery. The expression levels of *HIF-1α* and *NFκB* mRNA in the control group were increased at day 7 but decreased at day 25. Further, depletion of *CSDA* by shCSDA significantly upregulated the mRNA expression levels of these molecules at day 25 ($n=4$; Fig. 8B and C). Further, the mRNA expression levels of *VEGF-A*, *IL-6*, and the mouse IL-8 functional homolog, *CXCL2*, followed the changes in *HIF-1α* and *NFκB* mRNA ($n=4$; Fig. 9A–C). VEGF-A, IL-6, and CXCL2 secretions from muscle tissue were significantly increased in the shCSDA group compared with the control group at day 25 ($p<0.05$; Fig. 9D–F).

These data strongly suggest that RNAi targeting of CSDA could promote angiogenesis *via* the activation of HRE and NFκB-BE without direct transfer of angiogenic factors *in vivo*.

Discussion

In this study, we propose a novel mechanism for the neovascularization of ischemic skeletal muscle induced by muscle-derived angiogenic factors (Supplementary Fig. S4). We revealed that skeletal muscle has the potential to produce angiogenic factors (*i.e.*, VEGF-A, IL-6, and IL-8), but the secretion of these molecules is inhibited by a negative regulator of angiogenesis, CSDA, *via* repression of HRE and *NFκB-BE*. CSDA represses the secretion of angiogenic molecules (VEGF-A, IL-6, and IL8) from skeletal muscle and limits the paracrine effect of these molecules to endothelial cells. Further, RNAi targeting of CSDA was an effective therapy to enhance the potential of endogenous angiogenic molecules and to promote angiogenesis in a hindlimb ischemia mouse model.

CSDA (also known as dbpA) is a member of the Y-box-binding protein family (22) that is characterized by a common DNA/RNA-binding region called the CSD (31). CSD proteins have multiple functions, including the regulation of transcription and translation (14). CSDA can bind to CT-rich DNA sequences (26) (*i.e.*, HRE [3], G-CSF promoter [4], and SRE [20]). In the present study, we found that CSDA

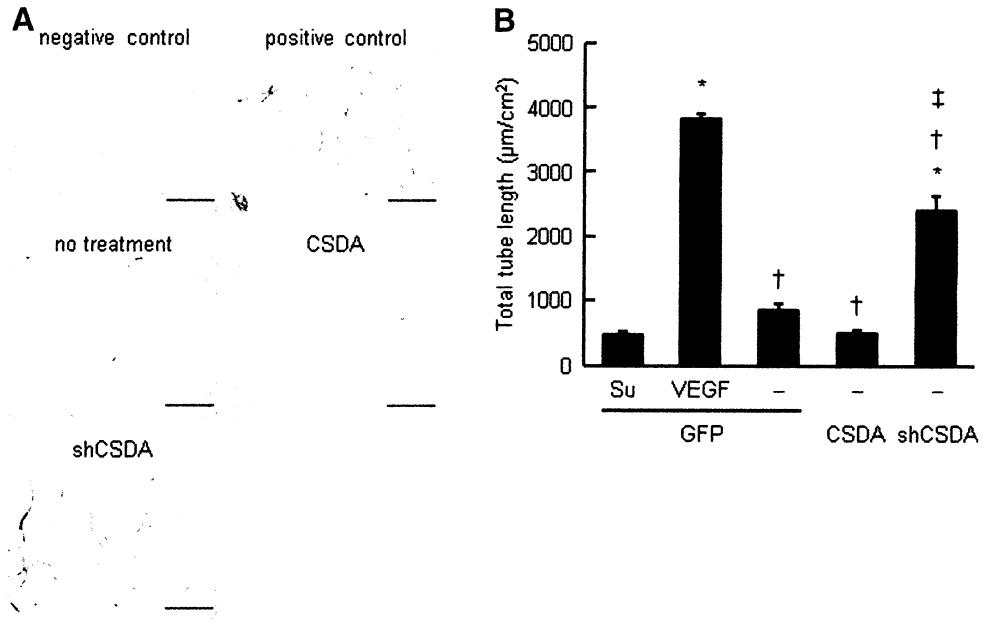

FIG. 6. CSDA induces *in vitro* angiogenesis. **(A)** Representative microscopic images of tube formation assay stained by CD31. Negative control: Cells were transfected with GFP and cultured in conditional medium with suramin (50 μM). Positive control: Cells were transfected with GFP and cultured in the medium with VEGF-A (10 ng/ml). No treatment: Cells were transfected with GFP and cultured in conditional medium only. CSDA: Cells were transfected with CSDA and cultured in conditional medium only. shCSDA: Cells were transfected with shCSDA and cultured in conditional medium only. Scale bar = 1 mm. **(B)** The total length of tube-like structures by an image analyzer. $n = 4$ different fields; $^{*}p < 0.05$ *versus* negative control; $^{\dagger}p < 0.05$ *versus* positive control; $^{\ddagger}p < 0.05$ *versus* no treatment.

can bind a new target, the NFκB-BE, and compete with NFκB to repress its activity. NFκB is the key regulator of many ILs and growth factors (*e.g.*, IL-6, IL-8, and granulocyte-colony stimulating factor), cytokines, cell adhesion receptors (*e.g.*, inter-cellular adhesion molecule-1 and vascular cell adhesion molecule-1), immunomodulatory proteins, and other proteins (*e.g.*, myosin heavy chains and matrix metalloproteinases) (5) and plays an important role in neovascularization. Further, NFκB mediates VEGF-A secretion *via* activation of HIF-1α (10, 19). Because NFκB is induced by VEGF-A (5), NFκB and VEGF-A form a positive autoregulatory loop. However, endogenous CSDA can repress both NFκB activity and VEGF-A secretion *via* independent mechanisms, and this synergistic activation of neovascularization is inhibited by CSDA. On the basis of these findings, we now recognize CSDA as a critical endogenous angiogenesis inhibitor.

The activities of many angiogenic factors have been investigated in many limb-ischemia animal models (8, 28). On the basis of these preclinical data, several angiogenic factors, including VEGF-A and fibroblast growth factor-2, have been tested in PAD patients (28). Despite claims of success in early, small, open-label trials, all double-blind, randomized, placebo-controlled trials reported to date have failed to conclusively show a clinical benefit (28). This difference between preclinical and clinical study results is a very important problem for therapeutic angiogenesis. Thus, a reasonable mechanism is required to explain this problem and to advance therapeutic efforts. Thus, we focused on control of the local balance between angiogenesis stimulators and inhibitors to achieve clinical benefits. On the basis of our results, we believe that CSDA is a critical endogenous angiogenesis inhibitor. The strategy of knocking down CSDA is reasonable for changing the local balance of angiogenic regulators, and it may be possible to improve upon classical gene therapy for PAD using this strategy. Further, an analysis of endogenous CSDA in PAD patients may help to determine a treatment strategy, especially to decide whether a PAD patient is a responder or nonresponder of angiogenic factors during the pretreatment assessment, which could increase the success of therapeutic angiogenesis.

The CSDA promoter region contains transcription factor-binding motifs for SRE, Sp-l, Oct-4, and the E-box (12). Interestingly, under normoxic conditions, the regulation of CSDA expression in skeletal muscle can be explained by the E-box sequence. MyoDl, which binds to the E-box, can regulate the gene expression of various muscle proteins, including myosin heavy chain, myosin light chain, and α-cardiac actin, in cooperation with the serum-response factor and Sp-l transcription factor (9, 15, 23). Our study demonstrated that CSDA was downregulated in the early ischemia phase *in vivo*, which resulted in the upregulation of HRE and NFκB-BE activity, which then increased the secretion of angiogenic factors. The rapid adaptation by the activation of HRE and the NFκB-BE during the acute phase was not sustained; in the late phase, CSDA expression was upregulated. Every growth factor was silenced, and finally, the original expression of CSDA was reversed by SRE self-regulation. These data suggest that CSDA is tightly controlled during hypoxic (ischemic) conditions as an endogenous angiogenesis inhibitor. CSDA knockdown appears to be a promising and novel gene therapy strategy to promote angiogenesis through the modulation of biological mechanisms.

In conclusion, the present study demonstrates that CSDA has a potent effect as an endogenous angiogenesis inhibitor in skeletal muscle and that RNAi targeting of CSDA appears to be a novel and promising strategy for improved gene therapy for PAD. We believe that the results of our present study will lead to new fields of research for angiogenesis and gene therapy development.

Materials and Methods

Cell culture

Human SkMCs were purchased from Lonza and maintained in skeletal muscle growth medium (Lonza) supplemented with 10% fetal bovine serum and skeletal muscle growth supplement (including rhEGF, insulin, GA-1000, fetuin, dexamethasone, and

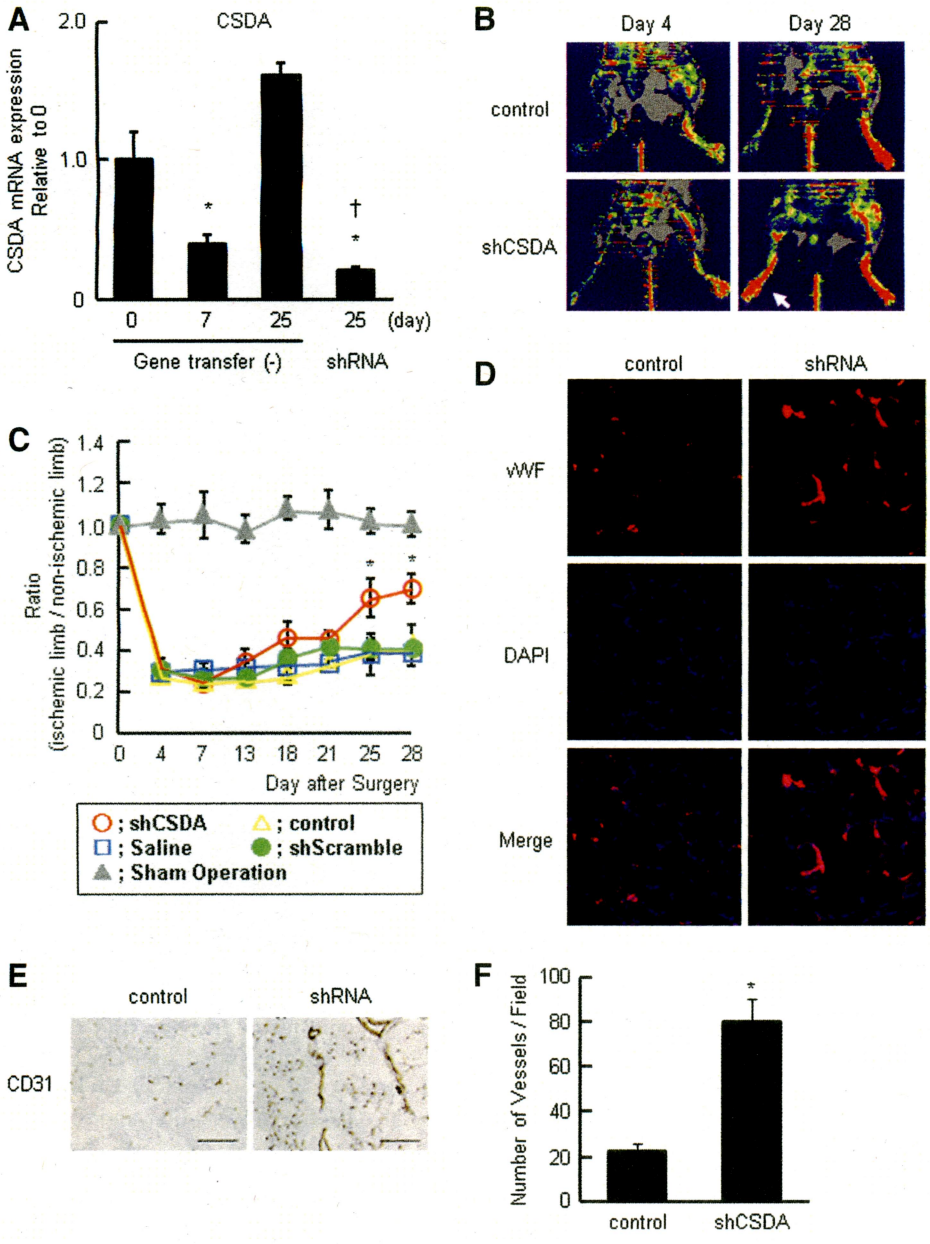

FIG. 7. Gene therapy with shRNA targeting CSDA induces angiogenesis *in vivo*. **(A)** Expression of endogenous CSDA of ischemic skeletal muscle tissue on days 0, 7, and 25 without gene transfer and day 25 with shCSDA transfer after surgery. $n=4$; $^{*}p<0.05$ *versus* 0 day; $^{\dagger}p<0.05$ *versus* 25 days without gene transfer. **(B)** Representative image of peripheral blood flow analyzed by LDI on days 4 and 28 after surgery. The left-side hind limb received surgery, and the right-side one was untreated. Color-coded images represent blood flow distribution; low or no perfusion is displayed as blue, whereas the highest perfusion is displayed as red *(white arrow)*. **(C)** Quantitative analysis of blood flow in hind limbs is expressed as the perfusion ratio of the ischemic hind limb to the untreated opposite limb on days 0, 4, 7, 13, 18, 21, 25, and 28 after surgery. $n=6$; $^{*}p<0.05$ *versus* every other group. **(D, E)** Representative image of immunofluorescence stains for vWF **(D)** or CD31 **(E)** in cross-sections of ischemic tissue at day 28. Scale bar = 100 μm. **(F)** Capillary density in cross-sections of ischemic tissue immunostained with CD31 antibody. $^{*}p<0.05$ *versus* control. LDI, laser Doppler imaging; shRNA, short-hairpin RNA; vWF, von Willebrand Factor.

bovine serum albumin). Cell quality was confirmed by immunofluorescence analysis (Supplementary Fig. S5). Cultures were incubated at 37°C in a humidified atmosphere of 95% air and 5% CO_2, and the medium was exchanged every 2 days. The cells at passages 5–8 were used in experiments. Hypoxic conditions were created using the AnaeroPack system (Mitsubishi Gas Chemical Company, Inc.), and cultures were incubated without changing the medium under continuous hypoxic conditions as measured by an anaerobic indicator (Becton, Dickinson and Company). The cells were transfected with the LipoTrust™ EX Gene reagent (Hokkaido System Science Co., Ltd.). Apoptosis was induced by actinomycin D (10 μM), camptothecin (2 μM), and etoposide (100 μM) according to the manufacturer's instructions (BioVision, Inc.).

Plasmid construct

The mouse CSDA plasmid was subcloned into the mammalian expression vector pcDNA3.1 (Invitrogen), which contains an influenza hemagglutinin tag (19). The pGeneClip™ Neomycin Vector (Promega), which expresses short-hairpin RNA (shRNA), was used for shRNA targeting of CSDA (shCSDA) and scramble (shSC) after inserting pairs of annealed DNA oligonucleotides. The sequence of the insert for the shRNA targeting CSDA (sense) was 5′-tctcGGA GAAACTG-TGAGTTTGATcttcctgtcaATCAAACTCTACAG TTTCTCCct-3′.

Real-time quantitative PCR

mRNA expression levels were measured by real-time quantitative PCR. Total RNA was extracted using Isogen (Nippon Gene). Complementary DNA was synthesized using the Thermo Script RT-PCR System (Invitrogen). Real-time quantitative PCR was performed using TaqMan Gene Expression Assays (human VEGF-A, Hs00900054; human HIF-1α, Hs00153153; human CSDA, Hs01124964; human NFκB, Hs00153294; human β-actin, 99999903; mouse VEGF-A,

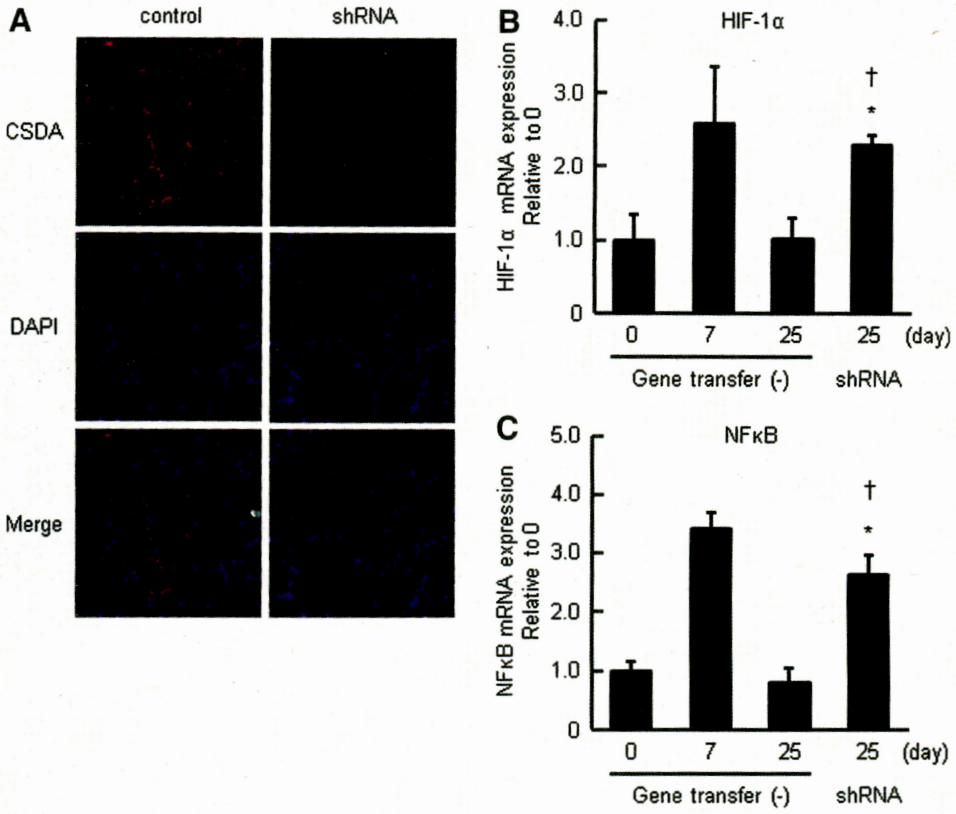

FIG. 8. HIF-1α and NFκB mRNA is upregulated by CSDA depletion *in vivo*. (A) Representative image of immunofluorescence stains for CSDA in cross-sections of ischemic tissue at day 28. Scale bar = 100 μm. **(B, C)** Expression levels of endogenous *HIF-1α* **(B)** and *NFκB* (p65) **(C)** of ischemic skeletal muscle tissue on days 0, 7, and 25 without gene transfer and on day 25 with shCSDA transfer after surgery. $n = 4$; $^{*}p < 0.05$ *versus* 0 day; $^{\dagger}p < 0.05$ *versus* 25 days without gene transfer.

Mm00437304; mouse HIF-1α, Mm00468869; mouse CSDA, Mm00516166; mouse NFκB, Mm00501346; mouse β-actin, Mm00607939; Applied Biosystems). The absolute number of gene copies was normalized using β-actin and standardized by a sample standard curve.

Western blotting

Nuclear extracts were prepared using NE-PER™ (Promega). Whole-cell lysates and nuclear extracts (40 μg) were resolved by SDS–polyacrylamide gel electrophoresis. Proteins were transferred onto a nitrocellulose membrane using iBlot™ (Invitrogen) and then incubated with primary antibody followed by an antirabbit immunoglobulin G-horseradish peroxidase secondary antibody (GE Healthcare UK Ltd.). Specific proteins were detected with enhanced chemiluminescence (GE Healthcare UK Ltd.). We used the following primary antibodies: VEGF-A (Santa Cruz Biotechnology, Inc.), HIF-1α (Invitrogen), CSDA (Aviva Systems Biology), phospho-specific or total NFκB (p65) (Cell Signaling Technology), LC-3 (Medical & Biological Laboratories Co., Ltd.), Atg-12 (Medical & Biological Laboratories Co., Ltd.), and actin (Sigma). To quantify and compare protein levels, the density of each band was measured by densitometry. Western blot of cytochrome *c* was performed using a Cytochrome *c* Releasing Apoptosis Assay kit (BioVision, Inc.) according to the manufacturer's protocol.

Evaluation of apoptosis and necrosis

We used the MitoCapture Apoptosis Detection kit (BioVision, Inc.) to detect disruptions in the mitochondrial transmembrane potential. To confirm differences between apoptosis and necrosis, we used a Green Fluorescence Protein (GFP)-Certified Apoptosis/Necrosis Detection kit (Enzo Life Sciences International, Inc.) according to the manufacturer's instructions. TUNEL labeling was performed using the *In Situ* Apoptosis Detection kit (Takara), according to the manufacturer's protocol, in combination with immunostaining for the appropriate cell marker. Counterstaining was performed using methyl green–pyronin. Propidium iodide (PI) staining was performed as previously described (17). Briefly, the cells were also stained with Hoechst 33258 (bisbenzimide, 10 *M*; Invitrogen) and PI (10 *M*; Sigma), because Hoechst 33258 stains all nuclei and PI stains the nuclei of cells with disrupted plasma membranes. The nuclei of viable, necrotic, and apoptotic cells were observed as blue intact nuclei, red round nuclei, and fragmented (or condensed) nuclei, respectively, under fluorescence microscopy.

VEGF promoter and NFκB assay

We determined the activity of the VEGF promoter and NFκB by cotransfecting cells with a luciferase reporter gene connected to the corresponding element (Clontech Laboratories, Inc.). Four hours after transfection, transfected cells were incubated with serum-free medium or conditioned medium. The cells were washed with phosphate-buffered saline and lysed for 5 min with 100 μl of cell lysis buffer at 37°C. Then, 20 μl of cell extract was mixed with 100 μl of luciferase assay reagent, and the light produced was measured for 30 s with a luminometer.

Enzyme immunoassay

The protein levels of human and mouse VEGF-A, human and mouse IL-6, human IL-8, and mouse CXCL2 were measured by

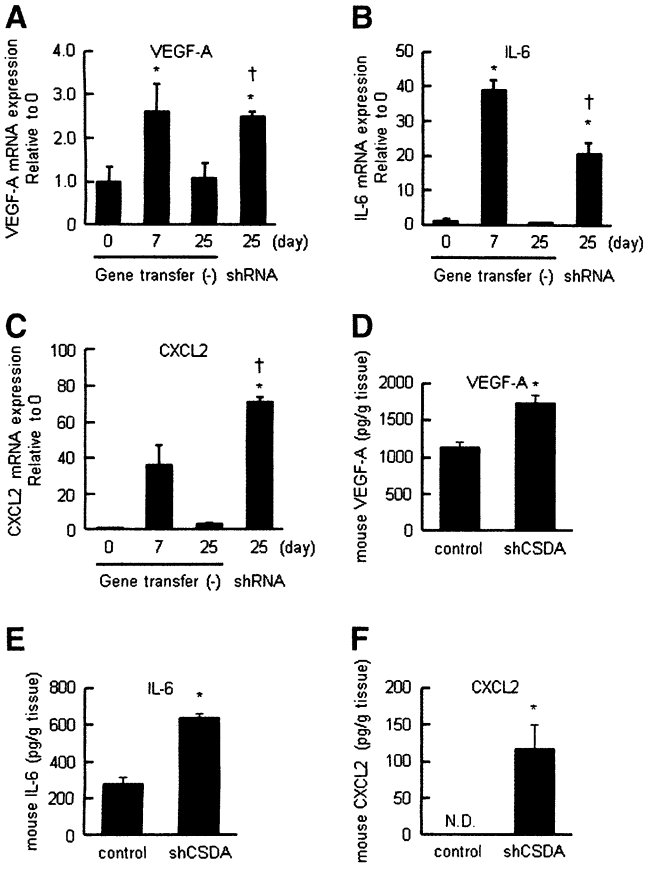

FIG. 9. Depletion of CSDA increases angiogenic molecule secretions *in vivo*. **(A–C)** Expression levels of endogenous VEGF-A **(A)**, IL-6 **(B)**, and IL-8 **(C)** of ischemic skeletal muscle tissue on days 0, 7, and 25 without gene transfer and on day 25 with shCSDA transfer after surgery. $n=4$; $^{*}p<0.05$ *versus* 0 day; $^{\dagger}p<0.05$ *versus* 25 days without gene transfer. **(D–F)** Effect of shCSDA on VEGF-A **(D)**, IL-6 **(E)**, and CXCL2 **(F)** secretion from ischemic skeletal muscle tissue at day 25 after surgery. $n=6$; $^{*}p<0.05$ *versus* control.

enzyme immunoassay (R&D Systems) according to the manufacturer's instructions (Invitrogen).

Immunofluorescence analysis

Immunofluorescence analysis was performed as previously described (21). The sections were stained with primary antibodies, including CSDA (Aviva Systems Biology), caspase 3 (Medical & Biological Laboratories Co., Ltd.), CD31 (Santa Cruz Biotechnology, Inc.), terminal deoxyribonucleotidyl transferase (Thermo Fisher Scientific Anatomical Pathology), NFκB (Santa Cruz Biotechnology, Inc.), von Willebrand Factor (Dako), actin (Abcam), myosin heavy chain (Abcam), desmin (Abcam), and MyoD1 (Abcam). Corresponding secondary antibodies were labeled with AlexaFluor555 or 488 (Molecular Probes).

Gel mobility shift analysis, competition, and antibody analysis

Nuclear extracts were prepared from cultured SkMCs with or without overexpressed CSDA using NE-PER (Promega). A gel retardation assay was performed using a Gel Shift Assay System (Promega) according to the manufacturer's instructions (with some modifications), a double-stranded NFκB-BE-consensus oligodeoxynucleotide, 5′-AGTTGAG GGG-ACTTTCCCAGGC-3′, and an NFκB-BE-mutant oligodeoxynucleotide, 5′-AGTTGAGGCGACTTTCCCAGGC-3′ (Santa Cruz Biotechnology, Inc.). Antibody experiments were performed by the addition of protein and NFκB antibody (Santa Cruz Biotechnology, Inc.), CSDA antibody (Aviva Systems Biology), or HA antibody (Santa Cruz Biotechnology, Inc.).

Tube formation assay

A human aortic endothelial cell tube formation assay was conducted in triplicate using an Angiogenesis kit (Kurabo) according to the manufacturer's instructions. Briefly, cells were transfected with CSDA, shCSDA, or GFP and cultured with or without VEGF-A (10 ng/ml) or suramin (50 μM) under normoxic conditions. After 10 days of incubation, the cells were stained with monoclonal antihuman CD31 antibody. The stained cells were photographed, and tubule-like structures in the images were analyzed for the length of tube formation using an Angiogenesis Image Analyzer (Kurabo).

Mouse hindlimb ischemic model and gene transfer protocol

All animal protocols were approved by the Animal Ethics Committee of Asahikawa Medical College. Wild-type male C57BL/6J mice were anesthetized with 1.5%–2.5% isoflurane in a mixture of air, and unilateral hindlimb ischemia was induced as previously described (24), with some modifications. Briefly, the common iliac artery near the aortic bifurcation, internal iliac artery, deep femoral artery, and superficial femoral artery were ligated, the ligated area was removed, and all side branches were dissected free. A total of 30 mice were randomly assigned to one of five groups: shCSDA plasmid (200 μg/0.1 ml; inserted on pGeneClip Neomycin Vector), GFP plasmid as a control (200 μg/0.1 ml; inserted on pcDNA3.1), saline (0.1 ml), shSC plasmid (200 μg/0.1 ml; inserted on pGeneClip Neomycin Vector), and sham operation. Plasmids or saline were injected intramuscularly using a 30-gauge needle on days 4, 7, 13, 18, 21, and 25 after surgery. Injected plasmids were transfected by a microbubble-enhanced ultrasound method as previously described (27). Blood flow was determined by LDI (Moor Instruments), and capillary density within the ischemic thigh adductor skeletal muscles was determined for the angiogenesis analysis (29).

Statistical analysis

All results are expressed as the means ± standard error of mean. Data were compared using the unpaired Student's *t*-test for comparisons between two groups. Analysis of variance followed by Dunnett's test was used for pairwise comparisons against the control, and Tukey's test was used for multiple comparisons. Differences were considered significant at $p<0.05$.

Acknowledgments

The authors thank Dr. Masakazu Haneda of Asahikawa Medical College for his support with the real-time quantita-

tive PCR analysis. This work was supported by a Grant-in-Aid for JSPS Fellows from the Japan Society for the Promotion of Science.

Author Disclosure Statement

No competing financial interests exist.

References

1. Arany Z, Foo SY, Ma Y, Ruas JL, Bommi-Reddy A, Girnun G, Cooper M, Laznik D, Chinsomboon J, Rangwala SM, Baek KH, Rosenzweig A, and Spiegelman BM. HIF-independent regulation of VEGF and angiogenesis by the transcriptional coactivator PGC-1alpha. *Nature* 451: 1008–1012, 2008.
2. Cao R, Brakenhielm E, Pawliuk R, Wariaro D, Post MJ, Wahlberg E, Leboulch P, and Cao Y. Angiogenic synergism, vascular stability and improvement of hind-limb ischemia by a combination of PDGF-BB and FGF-2. *Nat Med* 9: 604–613, 2003.
3. Coles LS, Diamond P, Lambrusco L, Hunter J, Burrows J, Vadas MA, and Goodall GJ. A novel mechanism of repression of the vascular endothelial growth factor promoter, by single strand DNA binding cold shock domain (Y-box) proteins in normoxic fibroblasts. *Nucleic Acids Res* 30: 4845–4854, 2002.
4. Coles LS, Diamond P, Occhiodoro F, Vadas MA, and Shannon MF. Cold shock domain proteins repress transcription from the GM-CSF promoter. *Nucleic Acids Res* 24: 2311–2317, 1996.
5. De Martin R, Hoeth M, Hofer-Warbinek R, and Schmid JA. The transcription factor NF-kappa B and the regulation of vascular cell function. *Arterioscler Thromb Vasc Biol* 20: E83–E88, 2000.
6. Eklund L and Olsen BR. Tie receptors and their angiopoietin ligands are context-dependent regulators of vascular remodeling. *Exp Cell Res* 312: 630–641, 2006.
7. Ferrara N. Vascular endothelial growth factor: basic science and clinical progress. *Endocr Rev* 25: 581–611, 2004.
8. Ferrara N and Alitalo K. Clinical applications of angiogenic growth factors and their inhibitors. *Nat Med* 5: 1359–1364, 1999.
9. Hennebry A, Berry C, Siriett V, O'Callaghan P, Chau L, Watson T, Sharma M, and Kambadur R. Myostatin regulates fiber-type composition of skeletal muscle by regulating MEF2 and MyoD gene expression. *Am J Physiol Cell Physiol* 296: C525–C534, 2009.
10. Jung YJ, Isaacs JS, Lee S, Trepel J, and Neckers L. IL-1beta-mediated up-regulation of HIF-1alpha via an NFkappaB/COX-2 pathway identifies HIF-1 as a critical link between inflammation and oncogenesis. *FASEB J* 17: 2115–2117, 2003.
11. Karst AM, Gao K, Nelson CC, and Li G. Nuclear factor kappa B subunit p50 promotes melanoma angiogenesis by upregulating interleukin-6 expression. *Int J Cancer* 124: 494–501, 2009.
12. Kudo S, Mattei MG, and Fukuda M. Characterization of the gene for dbpA, a family member of the nucleic-acid-binding proteins containing a cold-shock domain. *Eur J Biochem* 231: 72–82, 1995.
13. Martin D, Galisteo R, and Gutkind JS. CXCL8/IL8 stimulates vascular endothelial growth factor (VEGF) expression and the autocrine activation of VEGFR2 in endothelial cells by activating NFkappaB through the CBM (Carma3/Bcl10/Malt1) complex. *J Biol Chem* 284: 6038–6042, 2009.
14. Matsumoto K and Wolffe AP. Gene regulation by Y-box proteins: coupling control of transcription and translation. *Trends Cell Biol* 8: 318–323, 1998.
15. Minty A and Kedes L. Upstream regions of the human cardiac actin gene that modulate its transcription in muscle cells: presence of an evolutionarily conserved repeated motif. *Mol Cell Biol* 6: 2125–2136, 1986.
16. Moynagh PN. The NF-kappaB pathway. *J Cell Sci* 118: 4589–4592, 2005.
17. Nakagami H, Morishita R, Yamamoto K, Taniyama Y, Aoki M, Yamasaki K, Matsumoto K, Nakamura T, Kaneda Y, and Ogihara T. Hepatocyte growth factor prevents endothelial cell death through inhibition of bax translocation from cytosol to mitochondrial membrane. Diabetes 51: 2604–2611, 2002.
18. Remels AH, Langen RC, Gosker HR, Russell AP, Spaapen F, Voncken JW, Schrauwen P, and Schols AM. PPARgamma inhibits NF-kappaB-dependent transcriptional activation in skeletal muscle. Am J Physiol Endocrinol Metab 297: E174–E183, 2009.
19. Rius J, Guma M, Schachtrup C, Akassoglou K, Zinkernagel AS, Nizet V, Johnson RS, Haddad GG, and Karin M. NF-kappaB links innate immunity to the hypoxic response through transcriptional regulation of HIF-1alpha. *Nature* 453: 807–811, 2008.
20. Saito Y, Nakagami H, Kurooka M, Takami Y, Kikuchi Y, Hayashi H, Nishikawa T, Tamai K, Morishita R, Azuma N, Sasajima T, and Kaneda Y. Cold shock domain protein A represses angiogenesis and lymphangiogenesis via inhibition of serum response element. *Oncogene* 27: 1821–1833, 2008.
21. Saito Y, Nakagami H, Morishita R, Takami Y, Kikuchi Y, Hayashi H, Nishikawa T, Tamai K, Azuma N, Sasajima T, and Kaneda Y. Transfection of human hepatocyte growth factor gene ameliorates secondary lymphedema via promotion of lymphangiogenesis. *Circulation* 114: 1177–1184, 2006.
22. Sakura H, Maekawa T, Imamoto F, Yasuda K, and Ishii S. Two human genes isolated by a novel method encode DNA-binding proteins containing a common region of homology. *Gene* 73: 499–507, 1988.
23. Sartorelli V, Webster KA, and Kedes L. Muscle-specific expression of the cardiac alpha-actin gene requires MyoD1, CArG-box binding factor, and Sp1. *Genes Dev* 4: 1811–1822, 1990.
24. Sata M, Nishimatsu H, Suzuki E, Sugiura S, Yoshizumi M, Ouchi Y, Hirata Y, and Nagai R. Endothelial nitric oxide synthase is essential for the HMG-CoA reductase inhibitor cerivastatin to promote collateral growth in response to ischemia. *FASEB J* 15: 2530–2532, 2001.
25. Sato Y and Sonoda H. The vasohibin family: a negative regulatory system of angiogenesis genetically programmed in endothelial cells. *Arterioscler Thromb Vasc Biol* 27: 37–41, 2007.
26. Shannon MF, Coles LS, Vadas MA, and Cockerill PN. Signals for activation of the GM-CSF promoter and enhancer in T cells. *Crit Rev Immunol* 17: 301–323, 1997.
27. Shimamura M, Sato N, Taniyama Y, Yamamoto S, Endoh M, Kurinami H, Aoki M, Ogihara T, Kaneda Y, and Morishita R. Development of efficient plasmid DNA transfer into adult rat central nervous system using microbubble-enhanced ultrasound. *Gene Ther* 11: 1532–1539, 2004.
28. Simons M. Angiogenesis: where do we stand now? *Circulation* 111: 1556–1566, 2005.

29. Taniyama Y, Morishita R, Aoki M, Nakagami H, Yamamoto K, Yamazaki K, Matsumoto K, Nakamura T, Kaneda Y, and Ogihara T. Therapeutic angiogenesis induced by human hepatocyte growth factor gene in rat and rabbit hindlimb ischemia models: preclinical study for treatment of peripheral arterial disease. *Gene Ther* 8: 181–189, 2001.
30. Tateno K, Minamino T, Toko H, Akazawa H, Shimizu N, Takeda S, Kunieda T, Miyauchi H, Oyama T, Matsuura K, Nishi J, Kobayashi Y, Nagai T, Kuwabara Y, Iwakura Y, Nomura F, Saito Y, and Komuro I. Critical roles of muscle-secreted angiogenic factors in therapeutic neovascularization. *Circ Res* 98: 1194–1202, 2006.
31. Wolffe AP. Structural and functional properties of the evolutionarily ancient Y-box family of nucleic acid binding proteins. *Bioessays* 16: 245–251, 1994.

Address correspondence to:
Dr. Yukihiro Saito
Department of Surgery
Asahikawa Medical University
2-1 Midorigaoka-Higashi
Asahikawa
Hokkaido 078-8510
Japan

E-mail: y-saitou46@nifty.com

Date of first submission to ARS Central, October 22, 2010; date of final revised submission, April 2, 2011; date of acceptance, April 7, 2011.

Abbreviations Used

BE = binding element
CSD = cold shock domain
CSDA = cold shock domain protein A
DAPI = 4′,6-diamino-2-phenylindole
GFP = green fluorescence protein
HIF = hypoxia inducible factor
HRE = hypoxia response element
IL = interleukin
LDI = laser Doppler imaging
mRNA = messenger RNA
NFκB = nuclear factor κB
PAD = peripheral arterial disease
PI = propidium iodide
RNAi = RNA interference
shRNA = short-hairpin RNA
SkMC = skeletal muscle cell
SRE = serum response element
TUNEL = terminal deoxynucleotidyl transferase dUTP nick and labeling
VEGF = vascular endothelial growth factor